PASA Hand: A Novel Parallel and Self-Adaptive Underactuated Hand with Gear-Link Mechanisms

Dayao Liang, Jiuya Song, Wenzeng Zhang(✉), Zhenguo Sun, and Qiang Chen

Department of Mechanical Engineering, Tsinghua University, Beijing 100084, China
wenzeng@tsinghua.edu.cn

Abstract. This paper proposes a novel underactuated robotic finger, called the PASA finger, which can perform parallel and self-adaptive (PASA) hybrid grasping modes. A PASA hand is developed with three PASA fingers and 8 degrees of freedom (DOFs). Each finger in the PASA hand has two joints, mainly consists of an actuator, an accelerative gear system, a spring, a parallel four-link mechanism and a mechanical limit. Two extra actuators in the palm of the PASA hand independently control the base rotation of two fingers. The PASA hand executes multiple grasping modes based on the dimensions, shapes and positions of objects: (1) a parallel pinching (PA) grasp for precision grasp like industrial grippers; (2) a self-adaptive (SA) enveloping grasp for power grasp like traditional self-adaptive hands; (3) a parallel and self-adaptive (PASA) grasping mode for hybrid grasp like human hands. The switch through different grasping modes is natural without any sensors and control. Kinematics and statics show the distribution of contact forces and the switch condition of PA, SA, and PASA grasping modes. Experimental results show the high stability of the grasps and the versatility of the PASA hand. The PASA hand has a wide range of applications.

Keywords: Robot hand · Underactuated finger · Parallel and self-adaptive grasp

1 Introduction

A human hand is the most flexible and stable gripper until now. It can both grasp small and flat objects by using its distal phalanges, and grasp large objects by enveloping all the phalanges. With many degrees of freedom (DOFs), a human hand can realize different grasp modes.

To imitate human hand, dexterous hands were designed and developed, which have many joints and driven by many motors. The Utah/MIT Dexterous Hand [1], Stanford/JPL Hand [2], DLR Hand [3] and Gifu hand II [4] are outstanding examples. Soft robot hands [5] are also highly researched.

However, due to the limitation of mechanical dimension and grasping force need, it is really difficult to develop a robot hand which has as many as grasping modes as human hand and large grasping force. Furthermore, the development of robot hands is also limited by control scheme and sensor system.

To deal with these difficulties, underactuated hands were developed. In the research area of robotic hands, the underactuated mechanism is defined as: the number of

N. Kubota et al. (Eds.): ICIRA 2016, Part I, LNAI 9834, pp. 134–146, 2016.
DOI: 10.1007/978-3-319-43506-0_12

actuators is less than the number of degrees of freedom (DOFs). Underactuated hands have been researched since 1970s. Many kinds of underactuated hands have been developed to match the different needs in industrial applications, such as SARAH hand [6], tendon mechanisms hand [7], multi-finger underactuated hand [8], passive adaptive underactuated hand [9], underactuated prosthetic hand [10], and coupled self-adaptive hand [11]. Some methods are also used to study underactuated hands, see [12–14].

Traditional underactuated hands successfully solve the difficulties of controlling; but they only have few grasping modes. Laval University developed an underactuated hand [15] which can both realize pinching grasp and enveloping grasp. This hybrid grasping mode is proved to be a great success in multiple grasping tasks. [15] presented another underactuated grasper with multiple grasping mode.

Hybrid grasping mode combines the flexibility of dexterous hands and the stability and simplicity of traditional underactuated hands. Therefore, it is a popular research direction nowadays. This paper introduces a parallel and self-adaptive underactuated finger with a novel gear-link mechanism. Depending on the dimension, position and shape of objects, before the contact force is applied on the proximal phalanx, it executes parallel motion. After the force is applied, it envelopes the object. If the force is applied on the distal phalanx, the parallel mechanism remains unchanged and executes a pinching grasp. Different from the existing hands with the hybrid grasping mode, the PASA finger uses one actuator to control two joints, uses underactuated mechanism to switch different grasping modes automatically.

The second part of this paper introduces the concept of the parallel and self-adaptive (PASA) underactuated hand; the third part analyzes the structure, grasping-force distribution and the condition of pinching grasp and enveloping grasp of the PASA hand; the forth part shows the experimental results of different grasping processes.

2 Concept of Parallel and Self-Adaptive Underactuated Hand

Self-adaptive underactuated hands are suitable for grasping many kinds of objects. But most of them are difficult to grasp objects which are thin or small, as they can only process an enveloping grasp. When the objects are thin or small, the point contacts between the objects and phalanges are not stable.

Pinching is a very common way to grasp objects for humans. It can hold objects tightly such as paper and coin. As pinching and enveloping have their own advantages, it will improve its versatility if a robotic hand has both these two grasping modes.

As Fig. 1 shows, the parallel and self-adaptive underactuated grasping mode is a hybrid of the traditional self-adaptive enveloping grasp and the pinching grasp. Depending on the dimension, position and the shape of objects, the finger with the parallel and self-adaptive underactuated grasping mode executes an enveloping grasp or a parallel pinching grasp. The SARAH hand [16] designed by Laval University used this hybrid grasping mode, which proves its high value for industrial and civil applications.

To realize this hybrid grasping mode, the turn point from pinching grasp to enveloping grasp is the key. Before the lower part of the finger touches the object, the distal phalange and the base should form a parallel mechanism. As long as a contact force

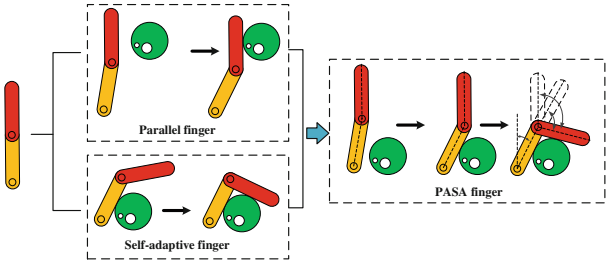

Fig. 1. Concept of parallel and self-adaptive underactuated finger.

applies on the lower part, the grasping mode transition is triggered, and a part of the parallel mechanism is fixed to the base. Hence, the parallel mechanism should be destroyed to execute an enveloping grasp. The next part of this paper will introduce the structure of a novel parallel and self-adaptive underactuated hand with gear-link mechanisms.

3 Architecture and Analysis of the PASA Hand

3.1 The Self-adaptive Rotation and Translation Systems of the PASA Finger

The translation system mainly consists of a parallel wheel, a link, a proximal phalanx, a distal phalanx, a gear set, a driving gear and a driven gear, which is fixed to the distal phalanx, as Fig. 2a shows. The driving force is transferred from the driving gear to the driven gear by the gear set. The connecting lines among the rotary axis of parallel wheel, proximal phalanx, link and distal phalanx form a parallelogram. If the parallel wheel does not rotate, the link keeps the distal phalanx always parallel to the last moment of the distal phalanx action.

The underactuated self-adaptive rotation system mainly includes a parallel wheel, a limiting block, a sliding block, a steel wire, a spring and an actuator. As it is shown in Fig. 2b, the sliding block is fixed to the parallel wheel and the limiting block is fixed to

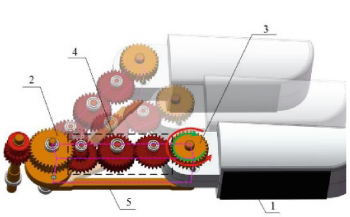

(a) Design of the underactuated translation system. 1-distal phalanx; 2- driving gear; 3-driven gear; 4-gear set; 5-link.

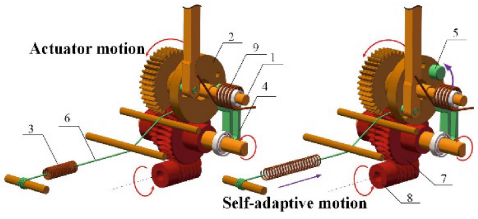

(b) Design of the underactuated self-adaptive rotation system. 1-proximal shaft; 2- parallel wheel; 3-spring; 4-limiting block; 5-sliding block; 6-steel wire; 7-worm wheel; 8-worm; 9- torsional spring.

Fig. 2. Architecture of the PASA Hand (Color figure online)

the base. One end of the steel wire is connected to the spring, the other end is connected to the parallel wheel. The driving force is transmitted to the driving gear through a worm, a worm wheel and other transmission mechanism. In the initial state, the sliding block abuts the limiting block by the force of spring. Once the proximal phalanx touches an object, the ensemble of gear set is stopped, but each gear continues rotating. The parallel wheel rotates in the direction of the purple arrow in Fig. 2b because of the translation system. As a result, a self-adaptive motion is produced while the actuator motion is taking place.

Based on the above analysis, take the ensemble of gear set as a reference system, the driven has two rotary directions: the green arrow direction in Fig. 2a (self-adaptive enveloping grasp) and the red arrow direction in Fig. 2a (parallel pinching grasp).

Figure 3 illustrates the function of the torsional spring. The torsional spring is added to enhance the grasping forces, which can also eliminate the effects of gear clearances.

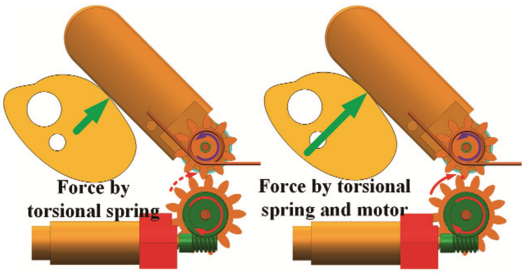

Fig. 3. Function of the torsional spring.

3.2 Integrated Design of the PASA Hand

The structure of the PASA finger is shown in Fig. 4. Each PASA finger mainly consists of a parallel wheel, a link, two phalanges, two shafts, a driving gear, a driven gear, a gear set, a sliding block, a limiting block, a spring and a torsional spring.

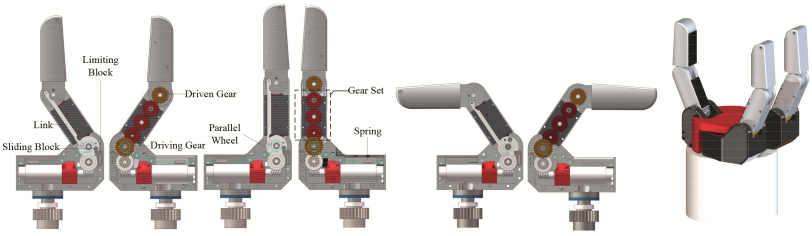

Fig. 4. The motion and structure of the PASA finger and the PASA Hand.

In the initial state, the sliding block contacts with the limiting block. The spring keeps the sliding block contact with the limiting block. The link keeps the distal phalanx always parallel to the last moment of the distal phalanx action since the sliding block is immobile.

As Fig. 4 shows, the proximal phalanx rotates forward since the driving gear rotates forward. The distal phalanx is parallel to the last moment of the distal phalanx because of the spring force, which is pinching process. Once the proximal phalanx touches an object, the driving gear continually rotates and drives the distal phalanx rotating forward. As a result, the parallel wheel rotates and the spring is strained, which is enveloping process.

3.3 Grasping-Force Distribution Analysis

This part focus on the grasping forces distribution of the PASA finger. For the reason of simplification, the gravity force of the finger and objects and the friction between phalanges are neglected, and the contact forces are applied on points.

As Fig. 5 shows, β is the rotary angle of the driving gear, θ_1 and θ_2 are the rotary angles of the proximal phalanx and the distal phalanx. The rotary angle of the parallel wheel is same as the distal phalanx because of the transmission link.

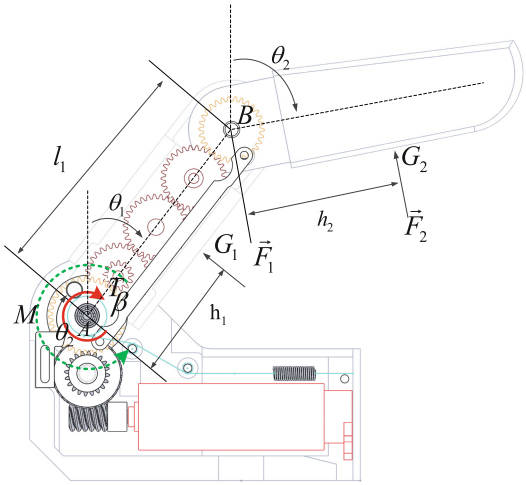

Fig. 5. Grasping-forces distribution analysis of the PASA finger.

The transmission ratio of the gear set is a. Take the proximal phalanx as a reference system, the rotary angles of the driving gear and driven gear are $\beta - \theta_1$ and $\theta_2 - \theta_1$. The relationship between these two angles is:

$$a(\beta - \theta_1) = \theta_2 - \theta_1 \tag{1}$$

Or

$$\theta_2 + (a-1)\theta_1 = a\beta \tag{2}$$

When the finger executes a pinching grasp, $\theta_2 = 0$, and θ_1 can be described as:

$$\theta_1 = a\beta/(a-1) \tag{3}$$

To realize a self-adaptive grasp, the rotary angle of proximal phalanx must be positive. One achieves $a > 1$.

As it is shown in Fig. 5, M and T are the torques produced by the spring and driving gear, $\vec{F}_1$ and $\vec{F}_2$ are the contact force vectors by the objects.

$$\vec{F}_1 = (-F_1 \cos\theta_1, F_1 \sin\theta_1) \tag{4}$$

$$\vec{F}_2 = (-F_2 \cos\theta_2, F_2 \sin\theta_2) \tag{5}$$

G_1, G_2 are the contact points. h_1 and h_2 are the distances between the contact points and the rotary axis. The vectors of the contact points $\vec{G}_1$, $\vec{G}_2$ can be described as

$$\vec{G}_1 = (h_1 \sin\theta_1,\ \mathrm{h}_1 \cos\theta_1) \tag{6}$$

$$\vec{G}_2 = (l_1 \sin\theta_1 + h_2 \sin\theta_2, l_1 \cos\theta_1 + \mathrm{h}_2 \cos\theta_2) \tag{7}$$

Since the rotary angle of the parallel wheel is also θ_2, the spring torque M is in direct proportion with θ_2. We use $k\theta_2 + M_0$ to represent M.

According to Lagrange's equation, one obtains

$$-\frac{\delta L}{\delta \vec{q}} = \vec{0} \tag{8}$$

Where

$$L = -V = -[-T, \frac{1}{2}k\theta_2 + M_0]\begin{bmatrix} \beta \\ \theta_2 \end{bmatrix} + [\vec{F}_1, \vec{F}_2]\begin{bmatrix} \vec{G}_1' \\ \vec{G}_2' \end{bmatrix} \tag{9}$$

Combine Eqs. (8) and (9), one achieves

$$[-T, k\theta_2 + M_0]\begin{bmatrix} \delta\beta \\ \delta\theta_2 \end{bmatrix} = [\vec{F}_1, \vec{F}_2]\begin{bmatrix} \delta\vec{G}_1' \\ \delta\vec{G}_2' \end{bmatrix} \tag{10}$$

Where

$$\delta\vec{G}_1 = (h_1 \cos\theta_{1,} - h_1 \sin\theta_1)\delta\theta_1 \tag{11}$$

$$\delta\vec{G}_2 = (l_1 \cos\theta_1\delta\theta_1 + h_2 \cos\theta_2\delta\theta_2, -l_1 \sin\theta_1\delta\theta_1 - h_2 \sin\theta_2\delta\theta_2) \tag{12}$$

$$\left[-T,\ \tau\theta_2 + M_0\right]\begin{pmatrix} \delta\beta \\ \delta\theta_2 \end{pmatrix} = \left[-T,\ k\theta_2 + M_0\right]\begin{bmatrix} \frac{a-1}{a} & \frac{1}{a} \\ 0 & 1 \end{bmatrix}\begin{bmatrix} \delta\theta_1 \\ \delta\theta_2 \end{bmatrix} \tag{13}$$

$$[\vec{F}_1, \vec{F}_2]\begin{pmatrix} \delta\vec{G}_1' \\ \delta\vec{G}_2' \end{pmatrix} = [F_1, F_2]\begin{bmatrix} -h_1 & 0 \\ -l_1\cos(\theta_2-\theta_1) & -h_2 \end{bmatrix}\begin{bmatrix} \delta\theta_1 \\ \delta\theta_2 \end{bmatrix} \tag{14}$$

Here we introduce two Jacobian matrix

$$\mathbf{J}_1 = \begin{bmatrix} \frac{a-1}{a} & \frac{1}{a} \\ 0 & 1 \end{bmatrix} \tag{15}$$

$$\mathbf{J}_2 = \begin{bmatrix} -h_1 & 0 \\ -l_1\cos(\theta_2-\theta_1) & -h_2 \end{bmatrix} \tag{16}$$

Finally, one obtains the relationship between spring force, driving force and contact forces:

$$[F_1, F_2] = [-T, k\theta_2 + M_0]\mathbf{J}_1\mathbf{J}_2^{-1} \tag{17}$$

Where

$$\mathbf{J} = \mathbf{J}_1\mathbf{J}_2^{-1} = \begin{bmatrix} -\frac{1}{h_1}(1-\frac{1}{a}-\frac{l_1\cos(\theta_2-\theta_1)}{ah_2}) & -\frac{1}{ah_2} \\ \frac{l_1\cos(\theta_2-\theta_1)}{h_1h_2} & -\frac{1}{h_2} \end{bmatrix} \tag{18}$$

From Eq. (18), one can study the relation between the contact forces and the distances of the contact points. As Fig. 6 shows, obviously, with the distances augment, the corresponding contact forces decrease.

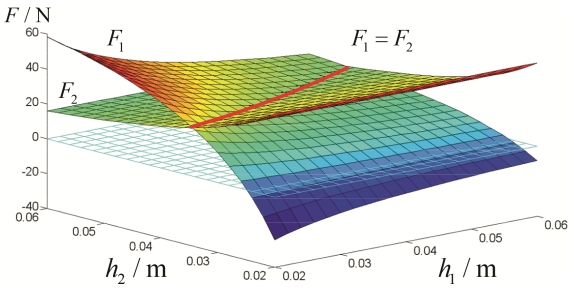

Fig. 6. Contact-force distribution by h_1, h_2, where $\theta_1 = 30^0, \theta_2 = 60^0, T = 3\text{N}\cdot\text{m}, a = 3, l_1 = 0.06\text{m}, M_0 = 0.006\text{N}\cdot\text{m}, k = 0.0344\text{N}\cdot\text{m}$.

The surfaces F_1 and F_2 intersect in a curve. It is almost a straight line, which means the contact forces are well-distributed.

If h_2 is too small, F_1 will become negative, which is an interesting phenomenon. Figure 7 shows this "retraction" phenomenon.

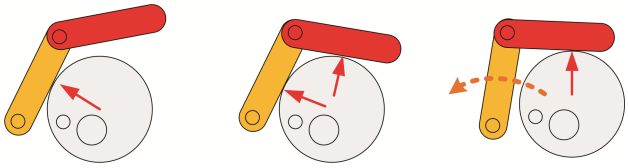

Fig. 7. "Retraction" phenomenon of a finger.

The forces distribution is also related to the rotary angles of two phalanges. If h_1, h_2, T, M_0, k, a, l_1 are fixed, F_2 has nothing to do with θ_1, and it only depends on θ_2. However, F_1 depends on both two rotary angles. As Fig. 8 shows, compared to F_1, F_2 is almost a constant.

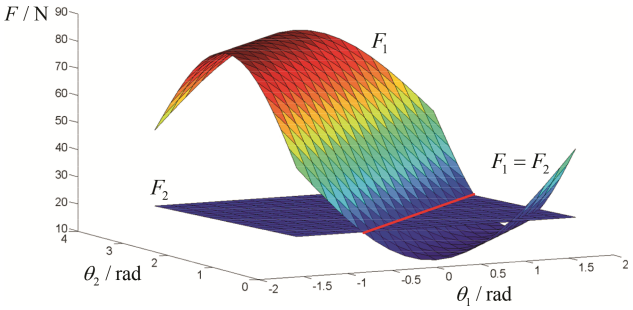

Fig. 8. Contact-force distribution by θ_1, θ_2, where $h_1 = 0.04\text{m}, h_2 = 0.04\text{m}, T = 3\text{N} \cdot \text{m}, a = 3, l_1 = 0.06\text{m}, M_0 = 0.006\text{N} \cdot \text{m}, k = 0.0344\text{N} \cdot \text{m}$.

In general, if θ_1 is small and θ_2 is large, F_1 is larger than F_2. Contrarily, if θ_1 is large and θ_2 is small, F_1 is smaller than F_2. (But not absolutely)

3.4 The Switch Condition of the Pinching and Enveloping Grasp

In order to find out the conditions where the parallel structure performs pinching motion, and the conditions where the parallel structure is switched to the enveloping motion, this part analyzes the static equilibrium when $F_1 = 0$ and $\theta_2 = 0$. As Fig. 9 shows, here $k\theta_2 + M_0$ is replaced by $-M'$, which is the contact torque between the limiting block and the sliding block.

Similar to the previous part, one obtains the expression of the contact forces:

$$F_1 = T\frac{1}{h_1}\left(1 - \frac{1}{a} - \frac{l_1\cos(\theta_2 - \theta_1)}{ah_2}\right) - M'\frac{l_1\cos(\theta_2 - \theta_1)}{h_1 h_2} \tag{19}$$

$$F_2 = T\frac{1}{ah_2} + M'\frac{1}{h_2} \tag{20}$$

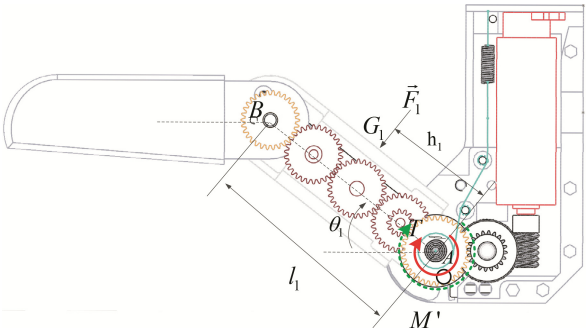

Fig. 9. Condition of pinching and enveloping grasp of the PASA finger.

Because $F_1 = 0$ and $\theta_2 = 0$, the contact torque between the limiting block and the sliding block can be described as

$$M' = T(1 - \frac{1}{a} - \frac{l_1 \cos\theta_1}{ah_2})\frac{h_2}{l_1 \cos\theta_1} \tag{21}$$

The condition where the parallel structure performs a pinching motion is $M' > 0$.
As a robotic hand, we limit $-90^0 < \theta_1 < 90^0$, $a > 1, T > 0$.
One achieves

$$h_2 > \frac{l_1 \cos\theta_1}{a - 1} \tag{22}$$

If h_2 satisfies Eq. (22), the PASA finger executes pinching grasp mode. Otherwise, the PASA finger executes enveloping grasp mode. This condition is determined by a, l_1 and θ_1, where a and l_1 is the system parameters and can be optimized. θ_1 changes once the size, shape and position of objects change.

$h_2 > l_1/(a-1)$ can be defined as a pinching zone and $h_2 < -l_1/(a-1)$ can be defines as an enveloping zone. In the interval $-l_1/(a-1) \le h_2 \le l_1/(a-1)$, the grasping mode changes according to the rotary angle of the proximal phalanx θ_1.

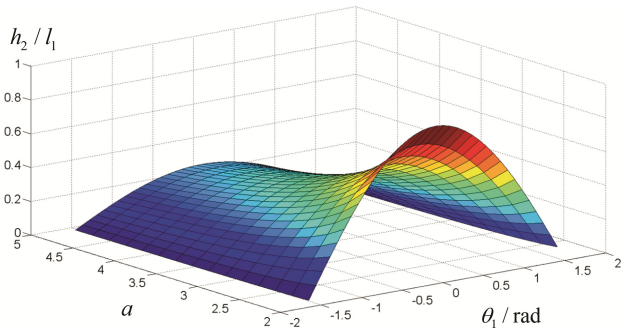

Fig. 10. Relation between h_2/l_1 and a, θ_1.

As a multi-grasping-mode finger, the pinching zone should not be too small, otherwise it will lose its practical significance. So parameter a should be much bigger than 1. For example, when $a = 3.5$, the pinching zone is $h_2 > 0.4l_1$.

Figure 10 shows the relation between h_1/l_1 and a, θ_1.

4 Experiments of the PASA Hand

To evaluate the performances of the PASA hand, this part conducts sevral experiments on the forces distribution, the influence of parameters and the versatility of the PASA hand.

As it is shown in Fig. 11, the prototype of PASA hand has three fingers, two of them can rotate around the arm. The actuators are ESCAP 16G214EMR19. The rotate speed of the driving gear is 10 r/min.

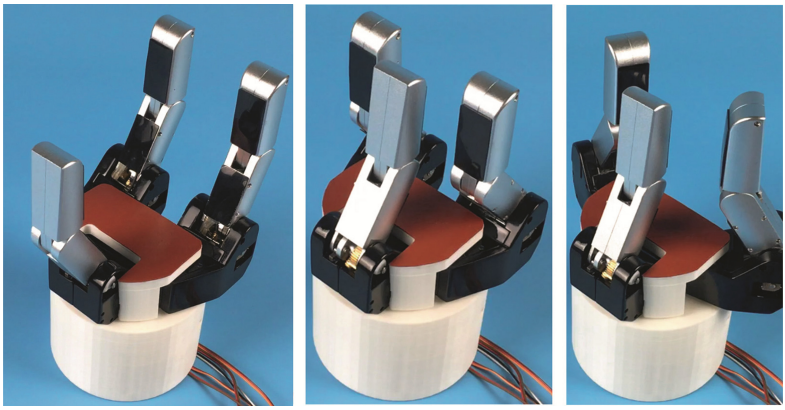

Fig. 11. The PASA hand.

4.1 Force Distribution

As a self-adaptive hand, the PASA hand envelopes objects when the force is applied on the proximal phalanx before the distal phalanx. If the contact force of the proximal phalanx is large but the distal phalanx doesn't contact the objects, the object will probably deform and the grasp is weak. So it is important to evaluate the contact force of the proximal phalanx when the distal phalanx begins to rotate. We call this force the "triggering force".

As Fig. 12a shows, the "triggering force" decreases when h_1 augments, which means larger objects are easier to envelope. It is also influenced by the rotary angle of the proximal phalanx.

Figure 12b shows the variation of the contact forces in an enveloping grasp process. After the distal phalanx rotates, the contact force of the proximal phalanx augments as the rotary angle of the distal phalanx becomes larger. When the distal phalanx comes into contact with the object, the contact force of the distal phalanx arguments instantly, and becomes larger than the contact force of the first phalanx.

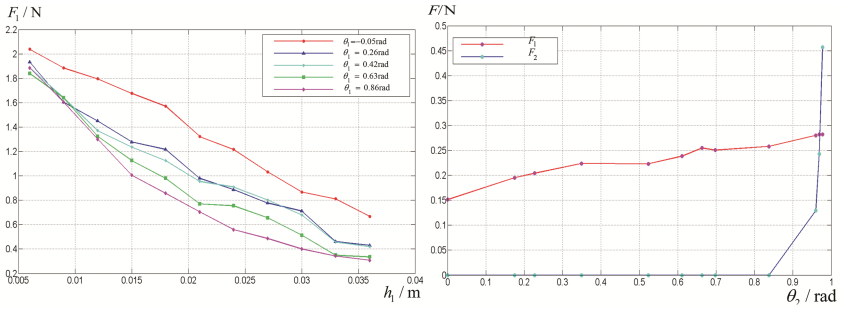

(a) Contact forces on the proximal phalanx when the distal phalanx begins to rotate.

(b) Contact forces after the distal phalanx rotates.

Fig. 12. Experiments of force distribution

4.2 Objects Grasping

To evaluate the versatility of the PASA hand, we use the PASA hand to grasp different objects. Depending on the objects, it executes pinching grasp or enveloping grasp automatically. When the object is located on the upper side of the finger, the PASA hand probably pinches it. When the object is large and located on the lower side of the finger, the PASA hand executes enveloping grasp. For some special objects, it can also execute pinching and enveloping grasps at the same time, as it is shown in the third picture of Fig. 13a.

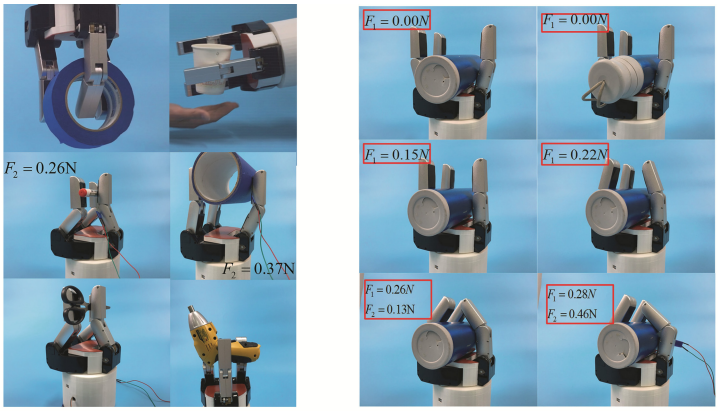

(a) Grasping experiments for different objects. (b) Grasping forces experiments.

Fig. 13. Experiments of different objects with the PASA hand.

Figure 13b shows three enveloping processes. The results show that the contact forces of the distal phalanx are larger than the contact force of the proximal phalanx when the enveloping processes are finished. A larger distal contact force will make the contact between the object and the base more stable.

5 Conclusions

This paper proposes a novel underactuated robotic finger (the PASA finger), which can perform parallel and self-adaptive (PASA) hybrid grasping modes. A PASA hand is developed with three PASA fingers and 8 degrees of freedom (DOFs). The PASA hand executes multiple grasping modes depending on the dimensions, shapes and positions of objects: (1) a parallel pinching (PA) grasp for precision grasp; (2) a self-adaptive (SA) enveloping grasp for power grasp; (3) a parallel and self-adaptive (PASA) grasping mode for hybrid grasp. Kinematics and statics show the distribution of contact forces and the switch condition of PA, SA, and PASA grasping modes. Experimental results show the high stability of the grasps and the versatility of the PASA hand. The PASA hand has a wide range of applications.

Acknowledgement. This Research was supported by National Natural Science Foundation of China (No. 51575302).

References

1. Jacobsen, S.C., Iversen, E.K., Knutti, D.F., et al.: Design of the Utah/MIT dextrous hand. In: Proceedings of the IEEE International Conference on Robotics and Automation, pp. 1520–1532 (1986)
2. Loucks, C.S.: Modeling and control of the stanford/JPL hand. In: 1987 International Conference on Robotics and Automation, pp. 573–578 (1987)
3. Butterfass, J., Grebenstein, M., Liu, H., et al.: DLR-hand II: next generation of a dextrous robot hand. In: IEEE International Conference on Robotics and Automation (ICRA), vol. 1, pp. 109–114 (2001)
4. Kawasaki, H., Komatsu, T., Uchiyama, K., et al.: Dexterous anthropomorphic robot hand with distributed tactile sensor: Gifu hand II. In: IEEE International Conference on Systems, Man, and Cybernetics (SMC), pp. 782–787 (1999)
5. Paek, J., Cho, I., Kim, J.: Microrobotic tentacles with spiral bending capability based on shape-engineered elastomeric microtubes, 01 August 2015. http://www.nature.com/srep/2015/150611/srep10768/abs/srep10768.html#supplementary-informationAB
6. Thierry, L., Gosselin, C.M.: Simulation and design of underactuated mechanical hands. Mech. Mach. Theor. **33**(1–2), 39–57 (1998)
7. Che, D., Zhang, W.: GCUA humanoid robotic hand with tendon mechanisms and its upper limb. Int. J. Soc. Robot. **3**(1), 395–404 (2011)
8. Zhang, W., Tian, L., Liu, K.: Study on multi-finger under-actuated mechanism for TH-2 robotic hand. In: IASTED International Conference on Robotics and Applications, pp. 420–424 (2007)
9. Zhang, W., Chen, Q., Sun, Z., et al.: Under-actuated passive adaptive grasp humanoid robot hand with control of grasping force. In: IEEE International Conference on Robotics and Automation (ICRA), pp. 696–701 (2003)
10. Massa, B., Roccella, S., Carrozza, M.C., et al.: Design and development of an underactuated prosthetic hand. In: IEEE International Conference on Robotics and Automation (ICRA), pp. 3374–3379 (2002)
11. Li, G., Liu, H., Zhang, W.: Development of multi-fingered robotic hand with coupled and directly self-adaptive grasp. Int. J. Humanoid Rob. **9**(4), 1–18 (2012)

12. Birglen, L., Gosselin, C.M.: Kinetostatic analysis of underactuated fingers. IEEE Trans. Robot. Autom. **20**(1), 211–221 (2004)
13. Birglen, L., Gosselin, C.M.: On the force capability of underactuated fingers. In: IEEE International Conference on Robotics and Automation (ICRA), pp. 1139–1145 (2003)
14. Birglen, L., Gosselin, C.M.: Geometric design of three-phalanx underactuated fingers. J. Mech. Des. **128**(1), 356–364 (2006)
15. Townsend, W.: The BarrettHand grasper – programmably flexible part handling and assembly. Ind. Robot Int. J. **27**(3), 181–188 (2000)
16. Demers, L.A., Lefrancois, S., Jobin, J.: Gripper having a two degree of freedom underactuated mechanical finger for encompassing and pinch grasping. US Patent US8973958 (2015)